

Application News

No.i245

Material Testing System

Evaluation of Temperature-Dependent Strength Properties of Lithium-Ion Battery Separator by Piercing and Tensile Testing

■ Introduction

Lithium-ion secondary cells, also called rechargeable batteries, (referred to here as "lithium-ion batteries") are widely used as energy sources for information terminals and consumer electronics, etc. because of their high energy density and cell voltage. Recently, their growing rate of dissemination into areas of general household applications, including hybrid and electric vehicles, is quite evident, and it appears obvious that the demand will further increase in the future.

Because lithium-ion batteries can sometimes become unstable due to short-circuit, over charging and discharging, impact, etc., a variety of protection mechanisms are incorporated at the battery component level to ensure safety.

Of these component parts, the lithium-ion battery separator prevents contact between the positive and negative electrodes, while at the same time playing a role as a spacer which permits the passage of lithium ions. However, it also performs the function of

preventing a rise in battery temperature due to excessive current in the event of a short circuit.

Because the lithium-ion battery separator is set in place so that it comes into contact with the rough surfaces of the positive and negative terminals, high mechanical strength is required. This mechanical strength must be maintained even if there is some rise in temperature, which is common to some degree, for example, during battery charging. Therefore, we conducted piercing and tensile testing measurements of the separator to evaluate changes in strength with respect to changes in temperature. This document introduces actual examples of these tests.

Supplement) Regarding the lithium-ion battery separator, previous evaluation examples were also introduced in Application News T146 "Measurement of Separator in Lithium-Ion Battery" and i229 "Multi-Faceted Approach for Evaluating Lithium-Ion Battery Separators."

■ Piercing Test

The samples consisted of separators removed from two lithium-ion batteries (cylindrical) used in small electrical devices, and we measured the changes in piercing characteristics due to changes in environmental

temperature. Fig. 1 shows an overview of the test conditions, and Table 1 presents details of the test conditions.

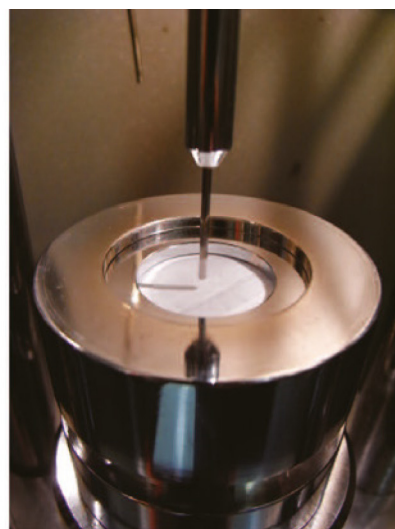
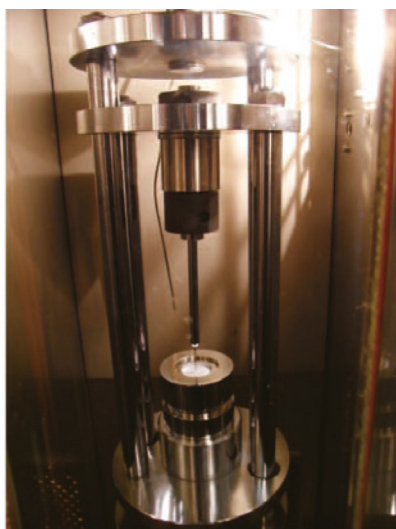
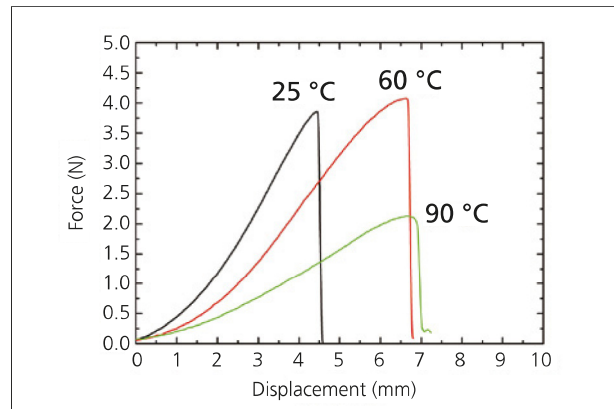


Fig. 1 Overview of Piercing Test

Table 1 Test Conditions (Piercing Test)

1) Instrument	Shimadzu AG-X Precision Universal Tester
2) Load cell capacity	1 kN
3) Jigs	Boil-in-bag piercing jig
4) Thermostatic chamber	TCR-1W
5) Load rate	50 mm/min
6) Temperature	25 °C, 60 °C, 90 °C
7) Software	TRAPEZIUMX (Single)

Fig. 2 shows the force – displacement curve, and Table 2 shows the maximum force and maximum displacement with respect to temperature. Comparing the test results at 25 °C and 60 °C, it is evident that there is not much difference in the maximum force, but the maximum displacement is greater at 60 °C. Comparing characteristic values at 60 °C and 90 °C, the decrease in maximum force is obvious at 90 °C, but the maximum displacement value is about the same. From the above, it can be assumed that at 60 °C, there is no decrease in strength of the lithium-ion battery separator, despite the apparent increase in its elongation property.

**Fig. 2 Test Result (Piercing Test)****Table 2 Summary of Results (Piercing Test)**

Temperature (°C)	Maximum Force (N)	Maximum Displacement (mm)
25	3.85	4.45
60	4.07	6.63
90	2.13	6.68

■ Tensile Test

The separators used for the tensile testing were removed from commercially available lithium-ion batteries (square-shaped), so 2 types of samples (below, referred to as samples (1) and (2)) which contained PE (polyethylene) as the principle constituent were used. When conducting the tensile tests, each separator

sample (as shown in Fig. 3(a)) was fashioned into dumbbell-shaped specimens oriented in the lengthwise and widthwise directions of each separator, as shown in Fig. 3(b). The total length of all specimen was 35 mm, with the parallel section measuring 10 (L) × 2 (W) mm.

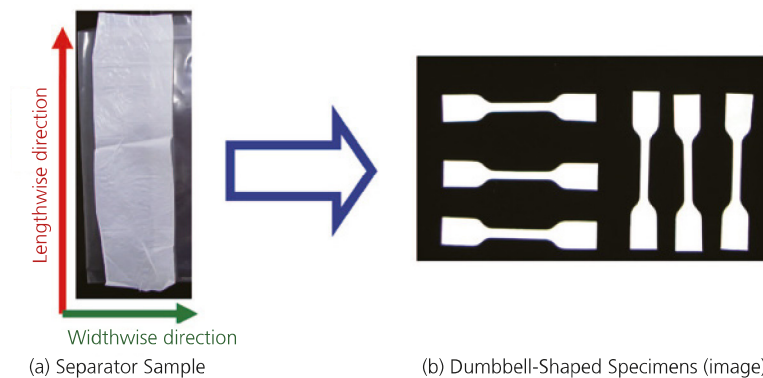
**Fig. 3 Test Samples**

Table 3 shows the tensile test conditions that were used.

Table 3 Test Conditions (Tensile Test)

1) Instrument	Shimadzu AG-X Precision Universal Tester
2) Load cell capacity	100 N
3) Jig	50 N capacity pneumatic flat grips (flat surface teeth, pneumatic pressure 0.4 MPa)
4) Thermostatic chamber	TCR-1W
5) Load rate	50 mm/min
6) Temperature	25 °C, 60 °C, 90 °C
7) Software	TRAPEZIUMX (Single)

Fig. 4 and Fig. 5 show the stress – strain curves for the widthwise and lengthwise directions, respectively of sample (1). Fig. 6 and Fig. 7 show the stress – strain curves for the widthwise and lengthwise directions, respectively of sample (2). Table 4 shows the test values of the mechanical properties obtained at each temperature.

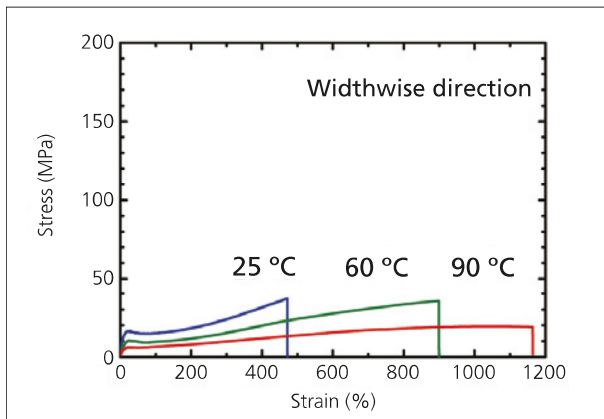


Fig. 4 Test Results (Sample (1), widthwise direction)

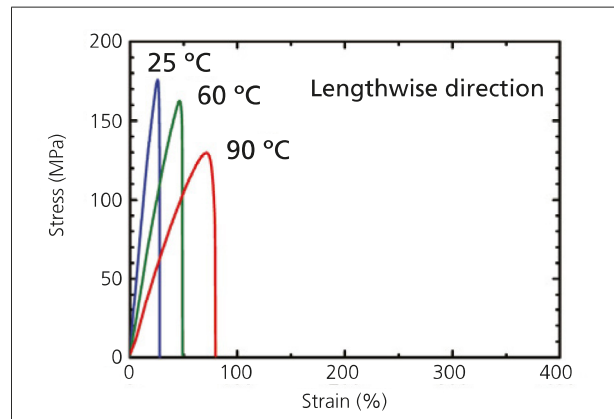


Fig. 5 Test Results (Sample (1), lengthwise direction)

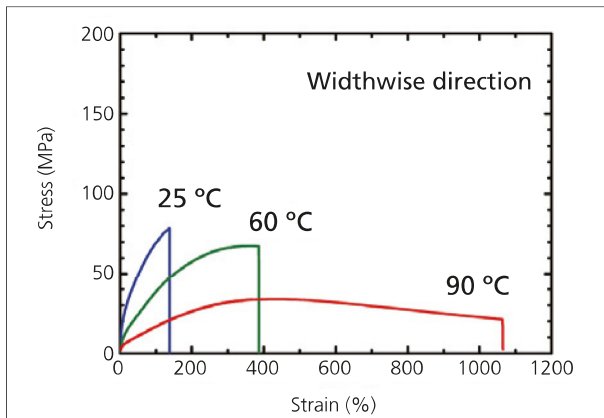


Fig. 6 Test Results (Sample (2), widthwise direction)

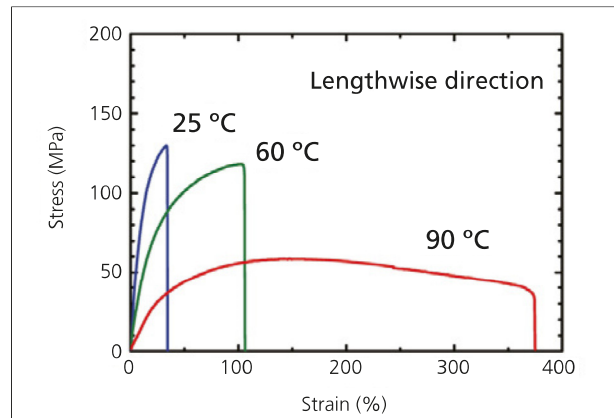


Fig. 7 Test Results (Sample (2), lengthwise direction)

Table 4 Summary of Results of Tensile Test

Sample	25 °C		60 °C		90 °C	
	Tensile Strength (MPa)	Strain at Break (%)	Tensile Strength (MPa)	Strain at Break (%)	Tensile Strength (MPa)	Strain at Break (%)
(1) Widthwise direction	36.9	471.4	35.4	898.8	19.3	1044.0
(1) Lengthwise direction	175.6	26.8	162.5	57.0	129.9	76.7
(2) Widthwise direction	78.2	138.5	68.8	347.6	33.8	427.9
(2) Lengthwise direction	129.5	34.1	118.3	105.3	58.7	367.2

In each of the samples, a lower tensile strength and greater elongation was seen in the widthwise direction than in the lengthwise direction. When comparing the numbers in Table 4, the lengthwise tensile strength for sample (1) is about 5 times greater than the widthwise tensile strength of sample (1). Also, the strain at break, for sample (1) in the lengthwise direction is lower by about a factor of 15 than that of sample (1) in the widthwise direction. From the above results, it is supposed that this separator (sample (1)) was manufactured using uniaxial drawing in the lengthwise direction. The widthwise tensile strength for sample (2) is about twice that of sample (1), and the strain at break is much lower. The tendency similar to that of sample (2) in the widthwise direction is seen with respect to sample (2) in the lengthwise direction. Therefore, due to the tendency of greater tensile strength and lower strain at break with sample (2) in the lengthwise direction, it is presumed that sample (2) was manufactured with a low biaxial drawing ratio, and that the drawing ratio in the lengthwise direction was greater than that in the widthwise direction. The data obtained regarding the mechanical properties with respect to the sample temperature are also

interesting. When comparing the sample strain at break and tensile strength at 25 °C and 60 °C, even though the strain at break value increased by a factor of 2 due to the test temperature increase to 60 °C, there was just a slight decrease in tensile strength. Similarly, when comparing the physical property measurement values at 60 °C and 90 °C, the strain at break showed the same tendency to greatly increase as when the values were compared at 25 °C and 60 °C. However, in this case, the tensile strength value shows a significant decrease. From the above, it is evident that the lithium-ion battery separators used in this test maintain excellent mechanical strength at 60 °C, notwithstanding its elevated elongation characteristics.

High-mechanical strength specifications are required for separators in order to withstand changing temperature in the cell. Here, as is clear from the results of piercing and tensile testing of lithium-ion battery separators under atmospheric temperature control, the mechanical properties of lithium-ion battery separators can be reliably evaluated using the Shimadzu Precision Universal Tester AG-X with its abundant array of accessories.